Journal of Luminescence 222 (2020) 117142

Contents lists available at ScienceDirect

Journal of Luminescence

journal homepage: www.elsevier.com/locate/jlumin

Full Length Article

Investigation of thermoluminescence processes during linear and isothermal heating of dosimetric materials

George S. Polymeris [a,1], Vasilis Pagonis [b,1], George Kitis [c,*,1]

[a] Institute of Nuclear Sciences, Ankara University, 06100 Beşevler, Ankara, Turkey
[b] McDaniel College, Physics Department, Westminster, MD 21157, USA
[c] Aristotle University of Thessaloniki, Physics Department, Nuclear Physics and Elementary Particles Physics Section, 54124 Thessaloniki, Greece

ARTICLE INFO

Keywords:
Thermoluminescence
Isothermal TL
LiF:Mg,Ti
BeO
Delocalized transition
Localized transition
Tunneling recombination

ABSTRACT

During experiments involving heating of dosimetric materials, trapped electrons are thermally excited and subsequently recombine with holes, producing a thermally stimulated luminescence signal. Thermal stimulation can take place either at a constant elevated temperature giving rise to a isothermal decay signal (PID), or with a constant heating rate which gives rise to a thermoluminescence (TL) signal.

The recombination pathways during thermal stimulation stage (also called the readout stage), can be either of a delocalized nature involving the conduction band, or of a localized nature involving an excited state of the trapped electrons. The present work investigates the experimental conditions which can distinguish between delocalized and localized transitions during the readout stage. The dosimetric materials used in this study are LiF:Mg,Ti, BeO, a natural apatite and artificial porcelain. The results show that during the readout stage with a constant heating rate, the prevalent recombination mechanism in all these materials involves delocalized transitions. However, the results show that during an isothermal decay experiment, the recombination mechanism in LiF:Mg,Ti and BeO involves delocalized transitions, whereas in the case of apatite and artificial porcelain the recombination takes place through localized transitions.

1. Introduction

Natural and artificial insulators contain impurities and crystal lattice defects, which give rise to localized energy levels within their forbidden band. Charged carriers created after irradiation with ionizing radiation can be trapped into long lived energy levels. Thermal stimulation of trapped electrons is followed by recombination with trapped holes, giving rise to thermally stimulated luminescence signals [1–5]. The energy required to liberate a trapped electron is termed the thermal activation energy E (eV). Three types of phenomenological models have been used extensively in the literature to describe the mechanisms involved in these processes: delocalized models based on transitions involving the conduction and valence bands, localized models usually involving different energy levels of the traps/centers, and semi-localized models based on a combination of localized and delocalized energy levels [1–9].

Thermal stimulation of trapped electrons can lead to two possible pathways to the luminescence center, either via a delocalized transition through the conduction band, or by a localized transition taking place from an excited energy level in the trap. These two possible pathways can of course coexist during an experiment, and are both characteristics of the dosimeter. When applying various methods of analysis, one does not know whether both pathways are involved; thus the two activation energies are unknown. In general, one expects that the E value for a localized process will be smaller than the activation energy for the delocalized process. Any differences observed between E values obtained with different methods of analyzing the experimental data are interpreted as the presence of both pathways in the luminescence process. Agreement between all methods of analysis is indicative of a single luminescence pathway.

Sfampa et al. [10] found that the prompt isothermal decay (PID) signals in Durango apatite shows a very weak dependence on temperature, contrary to the strong temperature dependence expected from conventional kinetic models. Similar effects were also observed in synthetic materials like magnesium tetraborate MgB_4O_7:Dy,Na (MBO) [11], in persistent luminescence phosphors $Sr_4Al_{14}O_{25}:Eu^{2+},Dy^{3+}$ [12] and during thermally-assisted optically stimulated luminescence experiments (TA-OSL) of Durango apatite [13].

In the case of both MBO [11] and $Li_2B_4O_7:Ag^{+},Gd^{3+}$[14] and $Sr_4Al_{14}O_{25}:Eu^{2+},Dy^{3+}$ [12] samples, a disagreement was found between

* Corresponding author.
E-mail address: gkitis@auth.gr (G. Kitis).
[1] All authors share an equal contribution in an indivisible way.

https://doi.org/10.1016/j.jlumin.2020.117142
Received 6 December 2019; Received in revised form 18 February 2020; Accepted 19 February 2020
Available online 20 February 2020

the activation energy E obtained using prompt isothermal decay methods (PID), and the values of E obtained using the initial rise and curve fitting methods for thermoluminescence (TL) signals.

From an experimental and theoretical point of view, it is important to establish techniques which can distinguish between delocalized and localized transitions, and also can distinguish between the different types of localized transitions. The goals of this paper are:

1. To investigate in a systematic manner whether it is possible to distinguish experimentally between the localized and delocalized transitions, for several well known dosimetric materials.
2. To compare the values of the activation energy E obtained from PID and TL experiments.
3. To compare the values of E obtained using different methods of analysis of TL data, namely the initial rise, PID and peak shape methods (PSM).
4. To discuss and explain the experimental data from the various materials, within the localized and delocalized transition models in the literature.

2. Materials and methods

2.1. Materials and apparatus

The materials used in the present work include (a) LiF:Mg,Ti, [2,4] square chips with dimensions 3 mm and thickness 1 mm purchased by Harshaw-Bicron. (b) BeO [15–18] square disks with dimensions of 4 mm and thickness of 1 mm purchased by Thermalox 995, Brush Wellman Inc., U.S.A. (c) natural Durango apatite [19] and (d) artificial dental porcelain [20]. All materials where in chip form except Durango apatite which was used in the form of grains with size 80-140 μm.

The above materials were selected for kinetic reasons described in the next Section 2.2, and for the stability and reproducibility of their thermally stimulated signals. Specifically, the TL and PID signals in these materials are found to be very stable and reproducible over many irradiation and readout cycles. This property allows the application of an experimental protocol in which a single aliquot of the sample is used. In addition, sensitivity tests are continuously applied during these experiments, to ensure the robustness of the results.

TL measurements for all materials were performed using a Thermo Scientific Harshaw TLD 3500 thermoluminescence system. The heating rate was selected at 1 °C/s and the maximum readout temperature 350 °C. The irradiations were performed using a ^{90}Sr-^{90}Y beta source, delivering 0.4 Gy/min at the irradiation set up.

2.2. Experimental protocol

The experimental procedure used for all materials is as follows:

Step 1: Irradiation with a test dose
Step 2: Pre-heat by a TL readout with a constant heating rate up to a temperature T_{pre}, in order to remove thermally unstable low temperature TL peaks. This preheating temperature varies upon the dosimetric material.
Step 3a: Increase the temperature by a TL readout with a constant heating rate up to a temperature where isothermal decay will take place T_{DEC} and record the signal.
Step 3b: Prompt isothermal decay at this T_{DEC} temperature for 150 s, recording the PID signal.
Step 4: TL readout up to the maximum allowed temperature, in order to obtain the remnant-TL signal (RTL). This is the TL signal remaining after the PID procedure in the previous step 3.
Step 5: Repeat steps 1 to 4 for a new increased isothermal decay temperature T_{DEC}.

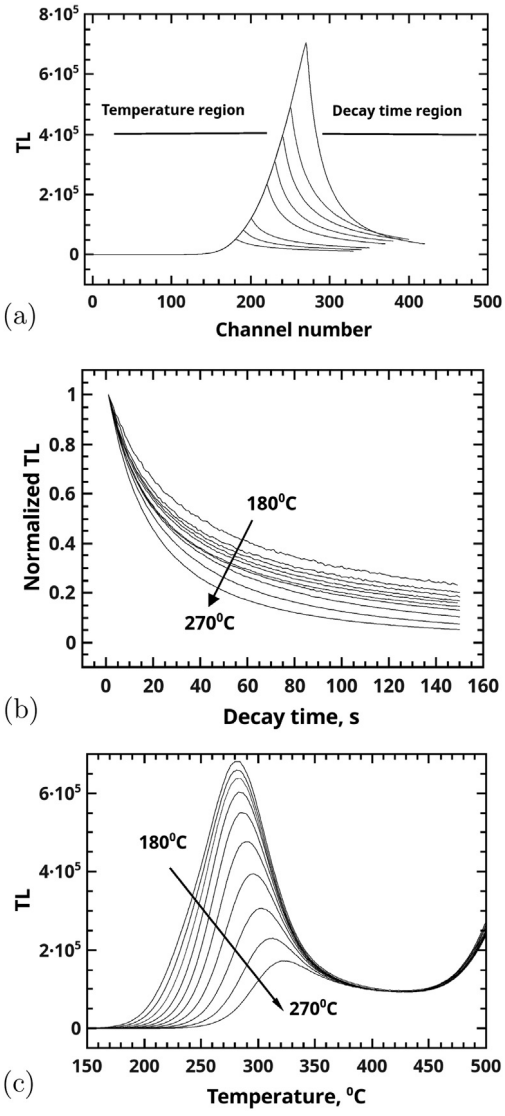

Fig. 1. Typical results from the experimental protocol taken from apatite sample. (a) PID measurements (b) The normalized PID curves from (a). (c) The RTL curves measured after the end of the isothermal decay procedure.

The above protocol requires good statistics, so the test dose in Step 1 was somewhat high, i.e. 0.5 Gy for LiF:Mg,Ti and BeO and 5 Gy for Durango apatite and porcelain.

âĂĺ The pre-heating temperatures in Step 2 for each material are: In LiF, 200 °C in BeO 140 °C, in apatite 180 °C and in porcelain: 180 °C.

Special care has been taken during the experimental protocol and during analysis of the data, to ensure that the thermal cleaning process does not produce any side effects to the main glow peak. The low temperature side of the TL signals is thermally cleaned in the protocol step 2. Concerning the high temperature side, the existing additional peaks in the glow curve are either of very low intensity and can therefore be ignored, or in some cases, this high temperature part is cleaned by an appropriate background subtraction. These cleaning methods are applied to a series of many TL glow curves and do not produce any appreciable changes in the main glow peak.

In order to provide a better description of this protocol, we show in Fig. 1 the results obtained for the apatite sample. Fig. 1a corresponds to Steps 3a and 3b of the protocol, which produce an increasing partial TL signal (Step 3a), followed by the decreasing prompt isothermal decay signal (PID).

The rising part of the signal measured in Fig. 1a is ideal for applying the initial rise method (IR), in order to evaluate the activation energy E. Since all measurements in Fig. 1a are part of the same TL glow peak, it is expected that the values of E obtained from the IR method will all be equal.

Fig. 1b shows all the PID curves obtained in Step 3b, normalized to the initial intensity at $t = 0$. Each one of these PID curves are fitted using the different analytical equations which are described in detail in the next section. The fitting of each isothermal decay curve gives the values of the isothermal decay constant λ. This decay constant depends on the temperature used during the PID experiment, according to an Arrhenius law $\lambda(T) = s\ exp(-E/kT_{dec})$, where (E, s) are the thermal activation energy and escape frequency characterizing the trap. By plotting the $\ln(\lambda(T))$ versus $1/kT$ for all decay temperatures, a linear plot is obtained with slope E. Under normal conditions, the resulting values of the activation energy E from this isothermal analysis, must be exactly equal with the values of activation energy obtained from the initial rise method.

The subsequent measurement in step 4 of the protocol gives the residual TL curves (RTL) shown in Fig. 1c, which represent the TL signal remaining after Step 2 and steps 3a and 3b in the protocol. These RTL curves are also used to evaluate the activation energy E, and one can expect these E values to be the same as the values of E evaluated from steps 3a and 3b. Both the initial rise method and the well-known peak shape methods (PSM) are applied to these RTL curves to evaluate the activation energy E.

In total, four different methods are used to analyze the PID and RTL data from each dosimetric material.

In all four dosimetric materials used in this study, the RTL glow curves contain a TL peak which is relatively isolated from satellite peaks. The term "main TL peak" will be used hereafter in the rest of this paper. In the case of LiF:Mg, Ti and BeO, the contribution of deeper traps to the high temperature part of the main TL peak is very low, so the peak can be considered isolated to a good approximation. In the case of apatite and porcelain, the peak isolation is relatively poor, as seen for example in Fig. 1c, in which the TL glow curves clearly contain peaks at higher temperatures above 400 °C. For these two materials, we use the following method to isolate the contribution of the main TL peak. At higher decay temperatures the trap has been emptied, so that the final RTL signal obtained, is in fact a background to the main TL peak, which can be subtracted from all previous RTL glow curves. This procedure of isolating the TL peak works very well for porcelain and apatite samples, because of the high repeatability of the RTL glow curves in the high temperature region, as seen in Fig. 1c.

2.3. Methods of analysis

The main quantities of interest in this study are the values of the activation energies E of the main TL peaks, obtained using the four different methods of analysis. Specifically, one might expect that the activation energy values E would be different for mechanisms involving delocalized transitions, and for those involving transitions between localized energy levels.

There are many methods for evaluation of the activation energy, and these are described in detail in textbooks [1,3]. In this study the methods used are:

- Initial rise method applied on the increasing luminescence signal shown for example in Fig. 1a.
- The isothermal decay method applied on the decaying the PID signals shown in Fig. 1b.
- The peak shape methods applied on the RTL signals shown in Fig. 1c.
- The initial rise methods applied on the RTL signals shown in Fig. 1c.

In the next subsections these methods are described in some detail.

2.3.1. Initial rise method

The initial rise (IR) method introduced by Garlick and Gibson [21] and simulated in detail by Kitis et al. [22], is the most valuable technique for the activation energy. It based on the suggestion that in the region of negligible disturbance of trap population the TL intensity will be given by:

$$I(T) = n_0\, s\, exp\left(-\frac{E}{kT}\right) \tag{1}$$

From Eq. (1) the plot of $ln(T)$ versus $1/kT$ is a straight line with a slope representing the activation energy $-E$.

In the present work the IR method was applied twice, to the RTL data in Fig. 1c, and to the increasing luminescence signal in Fig. 1a.

2.3.2. Prompt isothermal decay method

The decreasing PID curves in Fig. 1b can be described by different models as (a) A delocalized recombination model, (b) a localized recombination model and (c) a localized tunneling recombination model. Application of these three models to the experimental data is described in the next three subsections.

2.3.3. Delocalized recombination model

In the case of a delocalized model, the analytical expressions obtained from the solution of the one trap one recombination center (OTOR) model will be used. The original analytical expression for thermal decay at a stable temperature derived by Kitis and Vlachos [23] as a solution of the OTOR model is:

$$I(T) = \frac{N\,R}{(1-R)^2}\,\frac{\lambda}{W(z)+W(z)^2} \tag{2}$$

where N is the total concentration of electron traps, $W(z)$ is the Lambert W function [24] and $R = A_n/A_m$ with A_n the retrapping coefficient, A_m recombination coefficient and λ is the temperature dependent decay constant. As discussed above, this decay constant varies with the temperatureT_{dec} used during the PID experiment, according to $\lambda(T) = s\ exp(-E/kT_{dec})$.

Considering the case $R < 1$, re-trapping probability less than recombination probability, then Eq. (2) holds for the first real branch of the Lambert W function. The expression for z is given by

$$z = exp\left(\frac{R}{1-R} - ln\left(\frac{1-R}{R}\right) + \frac{\lambda t}{1-R}\right) \tag{3}$$

Previous simulation work has shown that Eqs. (2) and (3) are equivalent to what is known as the empirical general order kinetics decay [1,3].

These two equations are used to fit the experimental PID curves. The adjustable fitting parameters are the decay constant λ and the retrapping ratio R.

In this work the data is analyzed by using the Lambert W function. This function is chosen because it is the analytical solution of the single general one trap (GOT) differential equation, and can describe various shapes of the TL glow curves, ranging from first to second order kinetics. The GOT single differential equation is derived from the system of equations in the OTOR model, by applying the quasi-equilibrium conditions [23]. While there is no analytical solution for the system of differential equations in the OTOR

2.3.4. Localized transition model

Recently, Kitis and Pagonis [25] solved analytically the set of differential equations describing the localized transition model. The solution, given in terms of the Lambert W function, is:

$$I_{LOC}(t) = \lambda\,\frac{r}{W[z]+W[z]^2} \tag{4}$$

where the function z is given by:

$$z_{LOC-PID} = exp\left[\frac{r}{n_0} - ln\left[\frac{n_0}{r}\right] + \lambda t\right] \tag{5}$$

In these expressions n_0 is the initial concentration of trapped electron at time $t = 0$, and r is the retrapping ratio characterizing the localized transitions. $W(z)$ in Eq. (4) represents the first real branch of the Lambert W function. The adjustable fitting parameters in this localized model are the decay constant λ and the localized retrapping ratio r.

The Lambert function $W(z)$, is implemented in modern software packages as a built-in function, similar to any other transcendental function like sine, cosine etc. The Lambert function is termed ProductLog[(0,1),z] in Mathematica, Lambert w_0 and w_1 in MATLAB and EXCEL, gsl-sf-lambert-$w_0(z)$, gsl-sf-lambert-$w_1(z)$ in GNU GSL. w_0 and w_1 stands for the first and second real branch correspondingly.

In the present work the ROOT data Analysis Framework was used [26]. All fittings were performed using the MINUIT program [27] released in ROOT, which is a physics analysis tool for function minimization. The Lambert function $W(z)$ and the exponential integral function $Ei[-\frac{E}{kT}]$ are implemented in ROOT through the GNU scientific library (GNU GSL) [28].

2.3.5. Localized tunneling recombination model

Kitis and Pagonis [29,30] obtained analytical solutions of the set of differential equations in the model of Jain et al. [31], by using certain mathematical and physical simplifications. These authors presented analytical expressions describing thermally and optically stimulated luminescence signals within this model. The following analytical equation for TL glow curves was derived by these authors, within the framework of the tunneling recombination model by Jain et al. [31]:

$$L(T) = C A\, e^{-F(T)}\, e^{(-\rho'\,(F(T)^3))} \tag{6}$$

where the function $F(T)$ for TL processes is given by

$$F(T) = ln\left[1 + \frac{z\,\lambda\,k\,T^2}{\beta\,E}\,(1 - \frac{2k\,T}{E})\right] \tag{7}$$

with λ the temperature dependent decay constant, T is the temperature, β is the heating rate, $z = 1.8$ is a constant in the model, E is the activation energy, s is the frequency factor, k is the Boltzmann constant, ρ' a dimensionless parameter representing the dimensionless density of acceptors in the material.

For the case of isothermal decay, Eq. (6) becomes

$$L(t) = \frac{C\,F(t)^2\, e^{-\rho'(F(t))^3}}{1 + z\,\lambda t} \tag{8}$$

$$F(t) = ln\left(2.718 + z\,\lambda\,t\right) \tag{9}$$

The free fitting parameters of Eqs. (8) and (9) are the decay constant λ and the dimensionless density parameter ρ'.

2.3.6. Evaluation of the activation energy from the PID curves

The isothermal decay constant λ is evaluated with the above three methods [32] and is given by

$$\lambda = s\, e^{-\frac{E}{kT_{dec}}}, \tag{10}$$

where s (s^{-1}) the frequency factor, E (eV) the activation energy and T_{dec} is the PID temperature used in Step 3 of the experimental protocol. The value of λ is evaluated as a free parameter from the fitting procedure of the PID curves. As mentioned above,by plotting the $\ln(\lambda(T))$ versus $1/kT_{dec}$ for all decay temperatures, a linear plot is obtained with slope E.

2.3.7. Peak shape methods

The peak shape methods (PSM) are frequently used methods for evaluation of the activation energy E of an isolated TL peak. These methods were proposed by Chen [33–35] and are based on general order kinetics. Additional work on these methods was given by Kitis and Pagonis [36], and by Kitis et al. [37] for the case of mixed order kinetics. The PSM equations for the energy E are evaluated as the mean values obtained from a great number of (E, s) pairs [33,36,37].

The PSM are based on certain geometrical characteristics of a single glow-peak, namely the peak maximum temperature T_m and the temperatures T_1 and T_2 at half maximum TL intensity at the low and high temperature sides of the glow–peak, respectively. These quantities are used to define further the widths $\omega = T_1 - T_2, \delta = T_2 - T_m$ and $\tau = T_m - T_1$, as well as the symmetry factor of the glow-peak $\mu_g = \delta/\omega$.

The PSM equations used in this paper require also the values of TL intensity I_m at T_m, the total integral under the TL glow curve n_0, and the high temperature half integral under the TL glow curve n_m. Furthermore, instead of the geometrical symmetry factor μ_g, this paper uses the integral symmetry factor $\mu'_g = n_m/n_0$ [36,37].

There are three families of PSM equations, based on the widths ω, δ and τ. The PSM families of equations developed by Chen [33] and by Kitis et al. [36,37], give similar but not identical values of activation energy E. In the form used in this paper, the three PSM families give exactly the same values, and this is shown in Appendix. We will consider here only one of the three PSM equations, the one based on the width ω :

$$E_\omega = C_\omega \cdot \frac{1}{\mu'_g} \cdot b \cdot \frac{k\,T_m^2}{\omega} \tag{11}$$

where C_ω is the triangle assumption pseudo-constant [36] given by:

$$C_\omega = \frac{\omega\, I_m}{\beta\, n_0} \tag{12}$$

This constant can be evaluated from the experimental TL glow curves.

The value of the kinetic order b is necessary for this evaluation of E, and its value are evaluated from the following iterative expression proposed by Kitis and Pagonis [36,37]

$$\mu'_g = \frac{n_m}{n_0} = \left[\frac{b}{1 + (b-1)\Delta_m}\right]^{-\frac{1}{b-1}} \tag{13}$$

In the case of delocalized transitions, Kitis and Pagonis [38] showed that the general order kinetics order b can be, alternatively, evaluated from the expression:

$$b = \frac{W_1[f_{gen}\,\mu'_g\, ln(\mu'_g)]}{ln(\mu'_g)}\,. \tag{14}$$

$$f_{gen} = a_0 + a_1\,\mu_g'^{a_2}\,, \tag{15}$$

where a_0=0.965 ± 0.006, a_1=0.677 ± 0.09 and a_2=3.147 ± 0.02.

A numerical example of how the PSM equations are applied for the apatite sample, is as follows:

1. Extract from the TL peak the values of $I_m = 2.5 \times 10^5$, $n_o = 1.4 \times 10^7$, $n_m = 7.2 \times 10^6$.
2. Extract from the TL peak the values of $T_m = 539$ K, $\omega = 51$ K.
3. Evaluate the integral symmetry factor $\mu'_g = n_m/n_0 = 0.51$.
4. Evaluate the triangle assumption pseudo-constant $C_\omega = T_m\,\omega/n_0 = 0.904$, using Eq. (12).
5. Evaluate the kinetic order $b = 1.82$, using either Eq. (13), or Eq. (14).
6. Evaluate the activation energy $E_\omega = 1.76$ eV, using Eq. (11).
7. Evaluate the activation energies E_δ and E_τ, and these are found to be equal to $E_\omega = 1.76$ eV.

This example of applying the method is shown in Table 1.

As discussed above and proved in the Appendix, all three PSM families give the same value of E for the TL glow peak. An example of this agreement between the various methods is shown in Table 2.

Table 1
Example of evaluating the energy E using the peak shape methods.

Integral (a.u.)	Geometric	C_ω	μ_g'	b	E_ω
$I_m = 2.5\,10^5$	T_m= 266 °C (539 K)				
$n_0 = 1.4\,10^7$	$\omega = 51$ K	0.904	0.51	1.82	1.76
$n_m = 7.2\,10^6$	–				

Table 2
Case of LiF:Mg,Ti: Activation energy values E in eV, showing that the three peak shape methods based on ω, δ and τ give identical values.

Method	E_ω	E_δ	E_τ
PSM	2.3049	2.3049	2.3049
	2.0908	2.0908	2.0908
	2.4026	2.4026	2.4026
	2.4310	2.4310	2.4310
	2.4399	2.4399	2.4399

Table 3
Activation energy values in eV of all materials evaluated using the various methods described in the text.

Method	LiF	BeO	Apatite	Porcelain
PID (Deloc)	2.02 ± 0.07	1.26 ± 0.03		
PID (tun) C_1			0.21 ± 0.01	0.534 ± 0.03
PID (tun) C_2			0.70 ± 0.01	
PID (LocW) C_1			0.15 ± 0.005	0.32 ± 0.01
PID (LocW) C_2			0.33 ± 0.01	
I.R(ISO)	2.16 ± 0.1	1.22 ± 0.08	1.22 ± 0.07	1.17 ± 0.01
I.R(RTL)	2.45 ± 0.13	1.26 ± 0.03	1.63 ± 0.06	1.43 ± 0.07
PSM	2.34 ± 0.14	1.38 ± 0.08	1.75 ± 0.12	1.51 ± 0.14

3. Experimental results

3.1. LiF:Mg,Ti

The PID analysis to evaluate the temperature dependent decay constant $\lambda(T)$ were performed using Eqs. (2) and (3). The fitting of the PID data for this material was achieved by using a single value of the isothermal decay constant λ.

During the fitting procedure, the first 10 s of the PID signal are ignored, because this part of the signal rises with temperature before decaying at larger times, due to the sample arriving at thermal equilibrium. It is estimated that this small anomaly in the initial 10 s of the PID signal does not influence significantly the fitting process, and this part of the signal contributes only about 1% to the overall signal intensity.

The experimental results for LiF:Mg,Ti are shown in Fig. 2, and the activation energy values in Table 3. The PID curves shown in Fig. 2a show clearly the strong dependence on the decay temperature for this material. The activation energy E obtained from these curves is shown in Fig. 2b, and is equal to the E values obtained using the IR method, within experimental error.

Fig. 2c shows the corresponding RTL glow curves, from which new E values are derived by applying both the IR and the PSM equations. The resulting E values are slightly higher, but still in reasonable agreement with those obtained from the PID measurements.

The conclusion from this analysis is that the main peak 5 of LiF:Mg,Ti behaves exactly as expected according to a delocalized transition model.

3.2. BeO

The PID analysis to evaluate the temperature dependent decay constant $\lambda(T)$ were performed using Eq. (2), along with Eq. (3).

The experimental results for BeO are shown in Fig. 3a, and the activation energy values in Table 3. The PID curves in Fig. 3a show a very strong dependence on the isothermal decay temperature. The activation energy E resulting from these PID curves is shown in Fig. 3b, and is equal to the E values obtained by the IR analysis.

Fig. 3c shows the RTL glow curves, from which new values of E are obtained by using the IR method and the PSM equations. The resulting values are a bit higher, but in reasonable agreement with those obtained from the PID measurements, within experimental error.

The conclusion is that the main peak of BeO, just as the main peak 5 of LiF:Mg,Ti, behaves exactly as expected from a delocalized transition model.

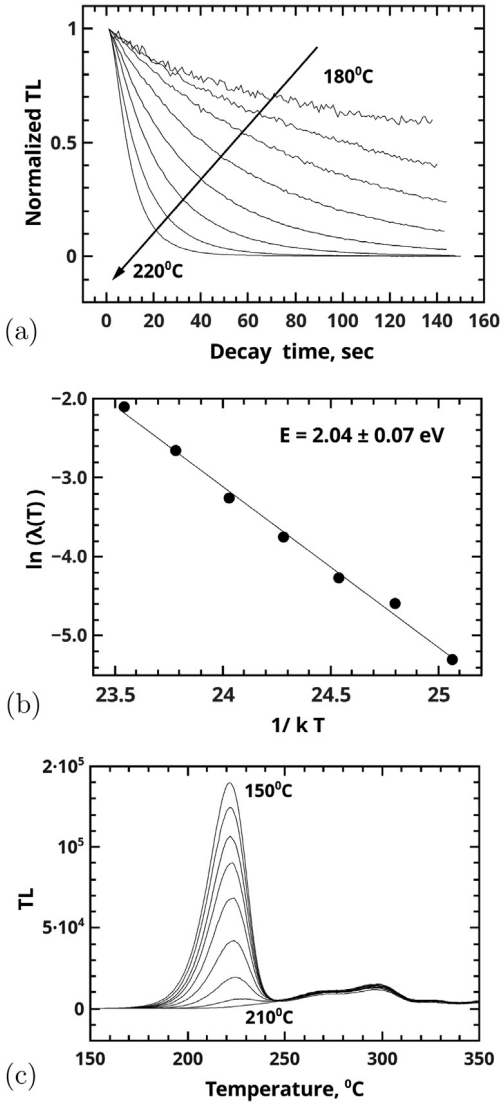

Fig. 2. Experimental data for LiF:Mg,Ti. (a) Normalized PID curves, (b) The activation energy obtained from the PID curves in (a), and (c) The RTL glow curves which are analyzed using the PSM.

3.3. Apatite

The experimental results for the Durango apatite sample are shown in Fig. 1. It is clear that the behavior of the PID curves of this sample in Fig. 1b is completely different from the corresponding behavior of LiF:Mg,Ti and BeO in Figs. 2 and 3. This is in agreement with previous experimental work by Sfampa et al. [10], who found that PID signals in Durango apatite show a very weak dependence on temperature, contrary to the strong temperature dependence expected from conventional delocalized kinetic models.

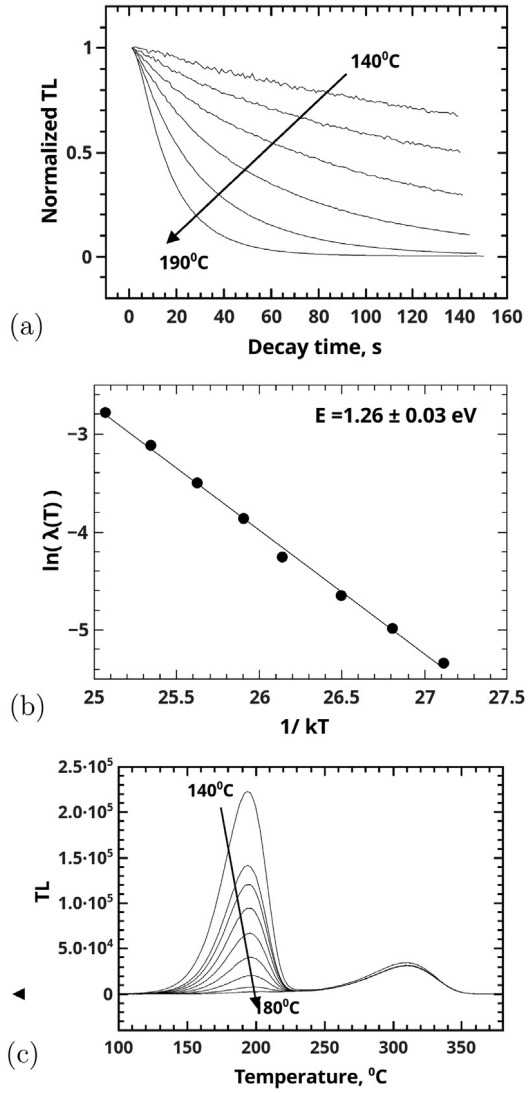

Fig. 3. (a) Normalized PID curves for BeO, (b) The activation energy obtained from the PID curves in (a), and (c) The RTL glow curves on which the PSM is applied.

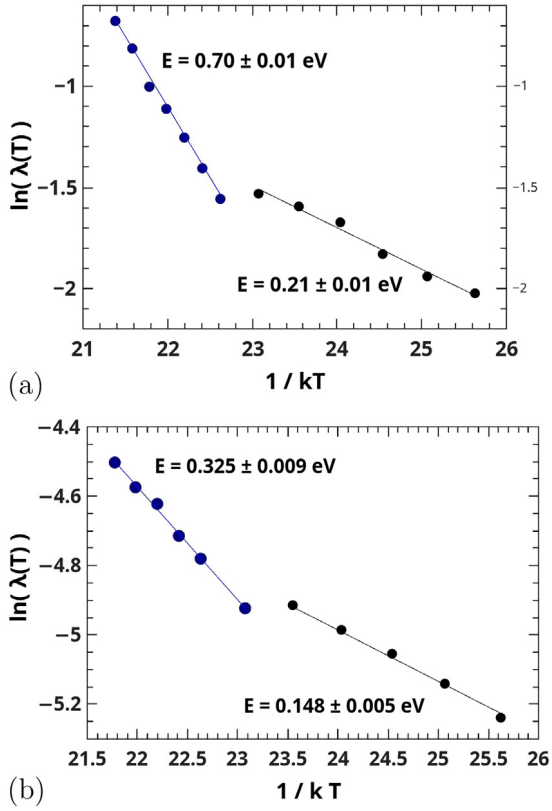

Fig. 4. Analysis of the PID data for Durango apatite, showing two components of the isothermal decay signals. (a) Results obtained using a tunneling recombination model and (b) Results obtained using a localized transition model. The models and equations are discussed in the text.

Based on this previous analysis of the PID data in this material, analysis of the PID data in this paper was carried out by using the two models of localized transitions described in the previous sections. Both localized transition models gave two sets of temperature dependent decay constants, leading to two different E values of the activation energy of the excited local energy levels. These two sets of E values obtained with the two localized transition models are shown in Fig. 4a,b. From this analysis, it is not possible to determine which of the two localized transition models is the correct one for this apatite.

More importantly, it is found that the activation energy value of $E = 1.22$ eV obtained from the IR analysis of the PID measurements, is much higher than the value of $E = 0.3$ eV obtained from the isothermal decay experiments. In addition, the E values obtained from the RTL glow curves are even higher, as shown in Table 3.

This large difference in the activation energy values, indicates that the thermal activation process taking place during readout with a linear heating rate, is different from the corresponding process taking place during the isothermal decay process.

The conclusion from this analysis is that as the temperature increases during a TL experiment with a linear heating rate, the luminescence process takes place via delocalized transitions, which require higher thermal energy. On the contrary, during the isothermal experiments for Durango apatite, localized transitions dominate the luminescence process, since these require lower amounts of thermal energy.

3.4. Porcelain

The experimental results concerning porcelain are shown in Fig. 5. The behavior of the PID curves of porcelain shown in Fig. 5a is similar to that of the Durango apatite, and completely different from the PID behavior of LiF:Mg, Ti and BeO. Therefore, the same type of analysis was used for the porcelain data in Fig. 5, as described previously for the apatite data. However, the porcelain data could be fitted with a single decay constant λ. The corresponding plots are shown in Fig. 6, and the activation energy values E are shown in Table 3.

The conclusion in the case of porcelain is exactly the same as for the Durango apatite data, i.e delocalized transitions take place during linear heating TL processes, and localized transitions dominate during the isothermal experiments.

4. Discussion and conclusions

A thermally stimulated electron can recombine through two basic pathways. In the first pathway, the electron is thermally excited to the conduction band and then recombines. This pathway is termed a delocalized transition. In the second possible pathway, the electron is excited thermally to a higher energy level within the forbidden gap, from which it recombines directly with a hole by either a tunneling transition or by direct de-excitation process.

According to the results in this work, the behavior of LiF:Mg,Ti and BeO is explained by using delocalized transitions, during both

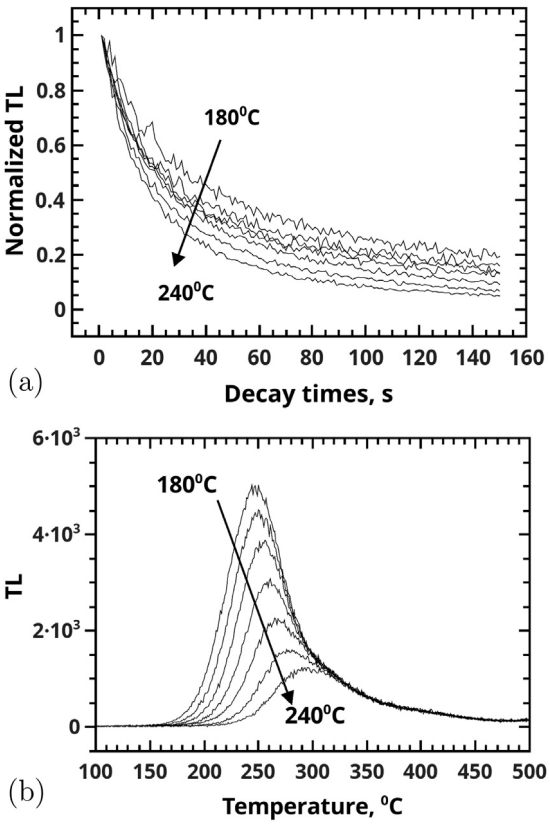

Fig. 5. Experimental data for porcelain sample (a) Normalized PID curves (b) The RTL glow curves on which the PSM is applied.

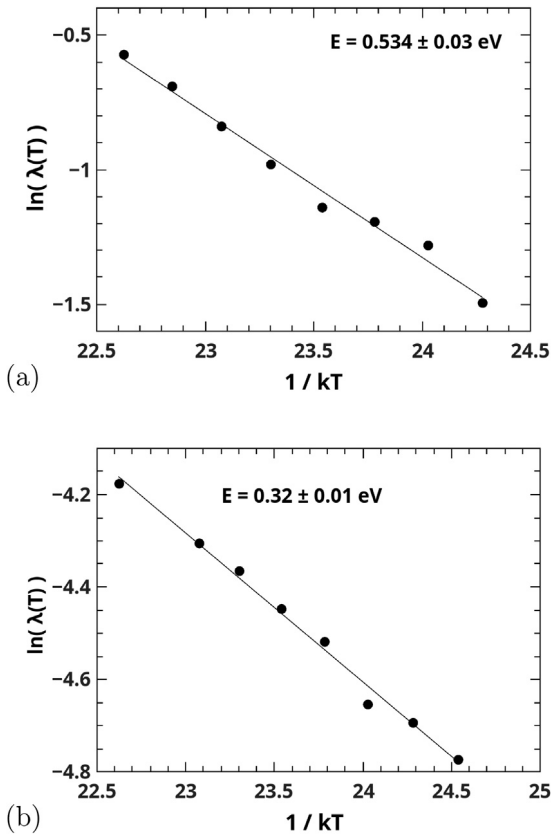

Fig. 6. Analysis of the PID data for porcelain sample, showing a single component of the isothermal decay signals. (a) Results obtained using a tunneling recombination model and (b) Results obtained using a localized transition model.

linear heating (readout), and during heating at a stable temperature (isothermal decay). We conclude that in these materials the recombination pathways is predominantly through the conduction band, and the luminescence mechanisms for the main TL peaks in these materials are clear representatives of delocalized transitions.

On the other hand the other two materials, Durango apatite and porcelain, showed a delocalized transitions behavior during linear heating (readout), but a localized transitions behavior during heating at stable temperature (isothermal decay).

In general, it is concluded that comparison of the PID and TL signals from a dosimetric material, can be a useful tool for distinguishing between luminescence mechanisms which involve localized vs delocalized transitions.

Declaration of competing interest

The authors declare that they have no known competing financial interests or personal relationships that could have appeared to influence the work reported in this paper.

Appendix

This Appendix shows that the following three PSM equations used in this work are equivalent.

$$\frac{\omega I_m}{\beta n_0} = C_\omega \tag{16}$$

$$\frac{\delta I_m}{\beta n_m} = C_\delta \tag{17}$$

$$\frac{\tau I_m}{\beta (n_0 - n_m)} = C_\tau \tag{18}$$

with

$$n_m = \int_{t_m}^{\infty} I\,dt$$

$$\frac{n_m}{n_o} = \mu'_g = \left[\frac{b}{1+(b-1)\Delta_m}\right]^{-\frac{1}{b-1}} \tag{19}$$

$$E_\omega = C_\omega \cdot \frac{1}{\mu'_g} \cdot b \cdot \frac{k T_m^2}{\omega} \tag{20}$$

$$E_\delta = C_\delta \cdot b \cdot \frac{k T_m^2}{\delta} \cdot b \cdot \frac{k T_m^2}{\tau} \tag{21}$$

$$E_\tau = C_\tau \cdot \frac{(1-\mu'_g)}{\mu'_g} \cdot b \cdot \frac{k T_m^2}{\tau} \tag{22}$$

$$\frac{E_\omega}{E_\delta} = \frac{C_\omega/\omega}{C_\delta/\delta}\frac{1}{\mu'_g} = \frac{I_m/n_0}{I_m/n_m}\frac{1}{\mu'_g} = \frac{n_m}{n_0}\frac{1}{\mu'_g} = \frac{\mu'_g}{\mu'_g} = 1 \tag{23}$$

$$\frac{E_\delta}{E_\tau} = \frac{C_\delta/\delta}{C_\tau/\tau}\frac{\mu'_g}{1-\mu'_g} = \frac{I_m/n_m}{I_m(n_0-n_m)}\frac{\mu'_g}{1-\mu'_g} = \frac{n_0-n_m}{n_m}\frac{\mu'_g}{1-\mu'_g} = \frac{1-\mu'_g}{\mu'_g}\frac{\mu'_g}{1-\mu'_g} = 1 \tag{24}$$

References

[1] R. Chen, Y. Kirsh, Analysis of Thermally Stimulated Relaxation Processes, Pergamon press, 1981.
[2] Y.S. Horowitz, Thermoluminescence and Thermoluminescence Dosimery, (Vol, I, II, III), CRS press, Boca Raton, 1984.
[3] R. Chen, S.W.S. McKeever, Theory of Thermoluminescence and Related Phenomena, World Scientific, 1997.
[4] Y.S. Horowitz, D. Yossian, Computerized glow curve deconvolution: Application to thermoluminescence dosimetry, Radiat. Prot. Dosim. 60 (1995) 1–114.
[5] G. Kitis, G.S. Polymeris, V. Pagonis, Int. J. Appl. Radiat. Isot. 153 (2019) 108797.

[6] A. Halperin, A.A. Braner, Evaluation of thermal activation energies from glow curves, Phys. Rev. 117 (1960) 408–415.
[7] R. Templer, The localized transition model of anomalous fading, Radiat. Prot. Dosim. 17 (1986) 493–497.
[8] R.K. Bull, Kinetics of the localized transition model for vthermoluminescence, J. Phys. D: Appl. Phys. 22 (1989) 1375–1379.
[9] A.J. Mandowski, Semi-localized transitions models for thermoluminescence, J. Phys. D: Appl. Phys. 38 (2005) 17–21.
[10] I.K. Sfampa, G.S. Polymeris, N.C. Tsirliganis, V. Pagonis, G. Kitis, Prompt isothermal decay of thermoluminescence in an apatite exhibiting strong anomalous fading, Nucl. Instrum. Methods Phys. Res. BV 320 (2014) 57–63.
[11] G. Kitis, G.S. Polymeris, I.K. Sfampa, M. Prokic, N. Meric, V. Pagonis, Prompt isothermal decay of thermoluminescence in $MgB_4O_7 : Dy, Na$ and $LiB_4O_7 : Cu, In$ dosimeters, Radiat. Meas. 84 (2016) 15–25.
[12] E. Karsu Asal, G.S. Polymeris, S. Gultekin, G. Kitis, Prompt isothermal decay properties of the $Sr_4Al_{14}O_{25}$ co-doped with Eu^{2+} and Dy^{3+} persistent luminescent phosphor, Nucl. Inst. Methods Phys. Res. B 425 (2018) 55–61.
[13] G. Kitis, G.S. Polymeris, V. Pagonis, N.C. Tsirliganis, Anomalous fading of OSL signals originating from very deep traps in Durango apatite, Radiat. Meas. 49 (2013) 73–81.
[14] A. Ozdemir, G.S. Polymeris, E. Sahiner, E. Aslar, V. Guckan, V. Altuna, N. Meric, Z. Yegingil, Evaluation of thermoluminescence trapping parameters in $Li_2B_4O_7$ co-doped with Ag^+ and Gd^{3+} using various experimental techniques, Nucl. Instrum. Methods Phys. Res. B 461 (2019) 70–76.
[15] G. Scarpa, The dosimetric use of beryllium oxide as a thermoluminescent material: A preliminary study, Phys. Med. Biol. 15 (1970) 667–672.
[16] E. Bulur, H.Y. Goksu, OSL from BeO ceramics: New observations from an old material, Radiat. Meas. 29 (1998) 639–650.
[17] M. Sommer, R. Freudenberg, J. Henniger, New aspects of a BeO-based optically stimulated luminescence dosimeter, Radiat. Meas. 42 (2007) 617–620.
[18] E.G. Yukihara, Luminescence properties of BeO optically stimulated luminescence (OSL) detectors, Radiat. Meas. 46 (2011) 580–587.
[19] G. Kitis, P. Bousbouras, C. Antypas, S. Charalambous, Anomalous fading in apatite, Nucl. Tracks Radiat. Measur. 18 (1991) 61–65.
[20] I.K. Sfampa, L. Malletzidou, P. Pandoleon, G. Kitis, Radiat. Meas. 125 (2019) 7–14.
[21] G.F.J. Garlick, A.F. Gibson, The electron trap mechanism of luminescence in sulfide and silicate phosphors, Proc. Phys. Soc. Lond. 60 (1848) 574–590.
[22] G. Kitis, V. Pagonis, E.E. Tzamarias, The influence of competition effects on the initial rise method during thermal stimulation of luminescence: A simulation study, Radiat. Meas. 100 (2017) 27–36.
[23] G. Kitis, N. Vlachos, General semi-analytical expressions for TL, OSL and other luminescence stimulation modes derived from OTOR model using the Lambert W function, Radiat. Meas. 48 (2013) 47–54.
[24] R.M. Corless, G.H. Gonnet, D.G.E. Hare, D.J. Jeffrey, D.J., D.E. Knuth, On the Lambert W function, Adv. Comput. Math. 5 (1996) 329–359.
[25] G. Kitis, V. Pagonis, Localized transition models: A reappraisal, Nucl. Instrum. Methods Phys. Res. B 432 (2018) 13–19.
[26] ROOT, A data Analysis Framework. https://root.cern.ch.
[27] MINUIT, A physics analysis tool for function minimization. Released in ROOT.
[28] GSL-GNU Scientific Library. www.gnu.org/software/gsl.
[29] G. Kitis, V. Pagonis, Analytical solution for stimulated luminescence emission from tunneling recombination in randomly distributions of defects, J. Lumin. 137 (2013) 109–115.
[30] V. Pagonis, G. Kitis, Properties of thermoluminescence glow curves from tunneling recombination processes in random distributions of defects, J. Lumin. 153 (2014) 118–124.
[31] M. Jain, B. Guralnik, M.T. Andersen, J. Phys. Condens. Matter 24 (2012) 385.
[32] M.L. Chithambo, P. Niyonzima, On isothermal heating as a method of separating closely collocated thermoluminescence peaks for kinetic analysis, J. Lumin. 155 (2014) 70–78.
[33] R. Chen, On the calculation of activation energies and frequency factors from glow curves, J. Appl. Phys. 40 (1969) 570–585.
[34] R. Chen, Glow curves with general order kinetics, J. Electrochem. Soc. 116 (1969) 1254–1257.
[35] R. Chen, S.A.A. Winer, Effects of various heating rates on glow curves, J. Appl. Phys. 41 (1970) 5227–5232.
[36] G. Kitis, V. Pagonis, Peak shape methods for general order thermoluminescence glow-peaks: A reappraisal, Nucl. Instrum. Methods Phys. Res. B 262 (2007) 313–323.
[37] G. Kitis, R. Chen, V. Pagonis, Thermoluminescence glow-peak shape methods based on mixed order kinetics, Phys. Status Solidi (a) 205 (2008) 1181–1189.
[38] G. Kitis, V. Pagonis, New expressions for half life, peak maximum temperature, activation energy and kinetic order of a thermoluminescence glow peak based on the Lambert W function, Radiat. Meas. 97 (2017) 28–34.